Available online at www.sciencedirect.com
ScienceDirect
Ceramics International 37 (2011) 2397–2403
CERAMICS INTERNATIONAL
www.elsevier.com/locate/ceramint

Improvement of mechanical properties of macroporous β-tricalcium phosphate bioceramic scaffolds with uniform and interconnected pore structures

Kaili Lin, Lei Chen, Haiyun Qu, Jianxi Lu, Jiang Chang *

State Key Laboratory of High Performance Ceramics and Superfine Microstructure, Shanghai Institute of Ceramics, Chinese Academy of Sciences, 1295 Dingxi Road, Shanghai 200050, PR China

Received 10 December 2010; received in revised form 18 January 2011; accepted 22 March 2011
Available online 1 June 2011

Abstract

The biocompatible and degradable macroporous bioceramic scaffolds with high mechanical properties and interconnected porous structures play an important role in hard tissue regeneration and bone tissue engineering applications. In this study, the improvement of mechanical properties of macroporous β-tricalcium phosphate [β-$Ca_3(PO_4)_2$, β-TCP] bioceramic scaffolds with uniform macropore size and interconnected pores were fabricated by impregnation of the synthesized β-TCP nano-powder slurry into polymeric frames. The microstructures, mechanical properties and *in vitro* degradation of the fabricated samples were investigated. For a comparison, β-TCP scaffolds were also fabricated from commercial micro-size powders under the same conditions. The resultant scaffolds showed porosities ~65% with uniform macropore size ranging from 400 to 550 μm and interconnected pore size ~100 μm. The compressive strength of the samples fabricated from nano-size powders reached 10.87 MPa, which was almost twice as high as those fabricated from commercial micro-size powders, and was comparable to the high-end value (2–10 MPa) of human cancellous bone. Furthermore, the degradation of the β-TCP bioceramics fabricated from nano-size powders was apparently lower than those fabricated from commercial micro-size powders, suggesting the possible control of the degradation of the scaffolds by regulating initial powder size. Regarding the excellent mechanical properties and porous structures, the obtained macroporous β-TCP bioceramic scaffolds can be used in hard tissue regeneration and bone tissue engineering applications.

Keywords: C. Mechanical properties; β-Tricalcium phosphate; Scaffolds; Porous structures; Nano-powders; Degradation

1. Introduction

The three-dimensional (3D) macroporous bioceramic scaffolds play an important role in hard tissue regeneration and bone tissue engineering. In tissue repair, these porous scaffolds serve as substrates for migration, proliferation, and differentiation of cells infiltrated from the surrounding tissues followed by the tissue ingrowths into the pores. These processes are affected by pore size, porosity and connectivity, etc. [1,2]. The *in vivo* studies had revealed that the volume of bone ingrowth increased with an increase of pore size. It has also been shown that pore diameters in the range of 150–500 μm can lead directly to mineralize bone [3,4]. Meanwhile, the macropore should be interconnected and the interconnections should be larger than 50 μm in diameter [5]. The well interconnected pore structures can significantly accelerate the vascularization and bone regeneration ability in clinical applications [6,7].

β-Tricalcium phosphate [β-$Ca_3(PO_4)_2$, β-TCP] bioceramics are wildly used for hard tissue regeneration due to their remarkable biocompatibility and their close chemical similarity to biological apatite present in human bones [8,9]. On the other hand, the β-TCP has been proved to be resorbable *in vivo* with new bone ingrowths replacing the implanted β-TCP. This property imparts significant advantage onto β-TCP compared to other biomedical materials, which are not resorbed and replaced by new-formed bone tissues [9,10]. Therefore, β-TCP bioceramics are widely used as bone replacements in the field of oral and plastic surgery and bone tissue engineering scaffolds [11–14].

* Corresponding author. Tel.: +86 21 52412804; fax: +86 21 52413903.
E-mail address: jchang@mail.sic.ac.cn (J. Chang).

0272-8842/$36.00
doi:10.1016/j.ceramint.2011.03.079

Besides the necessity of biocompatibility and 3D porous structures, the proper mechanical strength is required in order to maintain the shape against the stress during the surgical procedure and recovery. However, the mechanical strength of the scaffolds was usually low due to the high porosity, large macropore size and interconnected structures. The limitation of the scaffold strengths is one of the major challenges in the scaffold fabrication field. Similarly, the poor mechanical properties of β-TCP scaffolds have severely hindered their clinical applications [15–17]. For many years, a number of studies have been focused on the improving of mechanical strength of β-TCP bioceramics [15–20]. Recently, the concept of nano-technology has been applied to fabricate macroporous bioceramic scaffolds with significant improvement of the mechanical properties [15,21].

The aim of the present study was to fabricate the macroporous β-TCP bioceramic scaffolds with improved mechanical properties, and uniform macropore size and interconnected pore structures from nano-powders. Then the influence of the nano-size powders and commercial micro-size powders on the sintering, microstructure, mechanical properties and degradation of the scaffolds was investigated.

2. Materials and methods

2.1. Materials

The commercial micro-size β-TCP powders were obtained from Tomita (Tokushima, Japan). All other chemicals were obtained from China National Medicine Shanghai Chemical Reagent Corporation without further purifications.

2.2. Synthesis of nano-size β-TCP powders

The nano-size β-TCP powders for the present studies were synthesized by the reaction of $Ca(NO_3)_2$ with $(NH_4)_2HPO_4$. Briefly, 1000 mL of 0.4 mol $(NH_4)_2HPO_4$ solution with a pH about 8.0 was vigorously stirred at room temperature, and 1000 mL of 0.6 mol $Ca(NO_3)_2$ with a pH 8.0 was added drop wise over 300–360 min to produce a white precipitate. Throughout the mixing process the pH of the system was maintained at 8.0 ± 0.2 with the adding of ammonia solution. The white precipitate was then stirred for 24 h followed by washing with distilled water, and then washed with 100% ethanol to improve the dispersion characteristics. After washing, the remaining liquid was removed by vacuum filtration, and the precipitate was dried at 80 °C for 24 h. β-TCP was obtained by calcining the powders at 800 °C for 2 h with a heating rate of 5 °C/min.

2.3. Fabrication of macroporous β-TCP bioceramic scaffolds

The macroporous β-TCP bioceramic scaffolds with uniform macropore size and interconnected pores were fabricated by impregnation of β-TCP powder slurry into polymeric frames [22,23]. First, the polymeric frames with diameter 10 mm and height 12 mm were constructed by the polymethylmethacrylate balls (PMMA) in 500–600 μm sizes. The PMMA balls were poured into a metallic mould, and then the acetone was imported as the solvent to dissolve parts of the bodies and induced an overlapping between the individual bodies. This movement leads to the formation of necks between PMMA balls [22,23].

The synthetic nano-sized β-TCP powders and the commercial micro-size β-TCP powders were used as the starting raw materials to prepare the aqueous slurries with a powder concentration of ∼60 wt.%. Slurry defloculation (Darvan C, R.t. Vanderbilt Co.) was added in amount equals to 1.5 wt.% of β-TCP content. A quantity of organic binder (4 wt.% of β-TCP content, Duramax B1001, Rohm and Haas) was added to ensure a consolidation of green material during the polymer frame burnout. After a planetary milling for 1 h, the slurry was poured into plaster mould containing the polymeric frame. The plaster mould ensured the drying of material [22,23]. In the present study, the volume fraction of PMMA frames reached about 70% in the green samples. Therefore, the over-rapid heating rate would release large amounts of gas and generated intensively internal stresses due to the fast differential expansion between the polymer and the ceramic matrix. These phenomena might destruct the ceramic skeleton. To avoid this behaviour, the elimination of the PMMA frames was carried out by a mild thermal treatment at very slow heating rate of ∼0.1 °C/min [22,23]. The residual organic was then eliminated during a heating at 400 °C for 5 h. After this de-binding treatment, samples were sintered at 1100 °C or 1150 °C for 3 h in order to consolidate the ceramics.

2.4. Characterization of β-TCP powders and macroporous scaffolds

The morphology and size of the synthetic and commercially obtained β-TCP powders were observed by field emission transmission electron microscopy (FETEM: JEM-2100F, JEOL, Japan). XRD patterns of the β-TCP powders and scaffolds were characterized by X-ray diffraction (XRD: D/max 2550 V, Rigaku, Japan) with mono-chromated Cu Kα radiation at the scanning rate of 0.2°/min. The chemical composition of the synthesized and commercial β-TCP powders was analyzed by inductively coupled plasma atomic emission spectroscopy (ICP-AES; VISTA AX, Varian Co., USA). The porosity of the sintered samples was determined from the mass and dimensions of the sintered bodies [24,25]. The fracture surfaces of the sintered scaffolds were observed by field emission scanning electron microscope (FESEM: JSE-6700F, JEOL, Japan). The compressive strength of the fabricated samples was measured using a mechanical testing machine (Shimadza AG-5kN, Japan) with a loading rate of 0.5 mm/min. The elastic modulus was obtained automatically by the computer software in the testing machine, and the calculation was performed from the slope of the initial linear

portion of the compressive stress–strain curve based on the following equation:

$$\text{Elastic modulus} = \frac{ph}{\pi r^2 d}$$

where P is the applied load; r and h is the semi diameter and height of the samples, respectively; d is the displacement in the compressive test; π is the constant of 3.14. In this study, five samples from each group were tested to obtain average porosity, compressive strength and elastic modulus.

2.5. Soaking in Tris–HCl buffer solution

The degradation of the fabricated β-TCP bioceramic scaffolds was determined by their weight loss percentage in Tris–HCl buffer solution. The 0.1 M Tris–HCl buffer solution was prepared by dissolving analytical reagent grade Tris(hydroxymethyl) aminomethane in distilled water and then was buffered at pH 7.4 at 37 °C with hydrochloric acid. The samples were placed in polystyrene bottles containing Tris–HCl buffer solution. The bottles with the samples and Tris–HCl were maintained at 37.0 °C in a shaking water bath for 1, 3, 7, 14 and 21 days, respectively, for the degradation experiment, at the ratio of mass (g) to solution volume (mL) of 0.15 and refreshing the soaking medium every 24 h [26]. After various soaking periods, the samples were took out and rinsed with deionized water followed by drying in vacuum at 150 °C before further characterization. In this study, three samples from each group were tested to obtain an average degradation at each examining time.

3. Results and discussion

The morphology and size of the synthetic and the commercial β-TCP powders are shown in Fig. 1. It is clear to see that the two powders possessed quite distinctive characteristics in shape, size and size distribution. The synthetic β-TCP powders (Fig. 1A) showed less agglomerative morphologies and uniform particle size. The average particle size was about 100 nm, while the commercially obtained β-TCP powders (Fig. 1B) showed agglomerative morphologies and irregular particle shapes. The powder size distribution was in the wide range of between 0.5 and 2 μm. Table 1 shows the chemical composition of the synthetic nano-sized and the commercial micro-size β-TCP powders. It is clear to see that the impurity chemical composition of Mg and Fe in the commercial micro-size β-TCP powders was remarkably higher than those in the synthetic nano-sized powders. The Ca/P molar ratio of the synthetic nano-sized powders equal to the theoretic value of 1.50. However, the Ca/P molar ratio of the commercial micro-size powders only reached 1.47, which was slightly lower than theoretic value of 1.50.

Table 1
The chemical content of the synthetic and the commercial β-TCP powders.

Element content (wt.%)	Ca	P	Mg	Fe	Ca/P molar ratio
Commercial powders	39.41	20.72	0.0590	0.0016	1.47
Synthetic powders	39.48	20.38	0.0009	0.0004	1.50

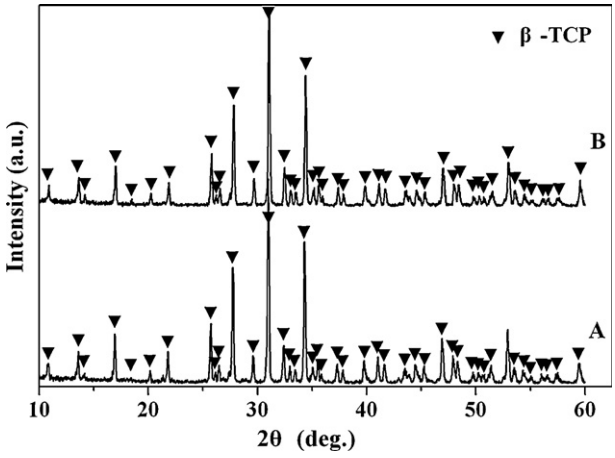

Fig. 2. XRD patterns of the synthetic nano-sized (A) and commercial micro-size (B) β-TCP powders.

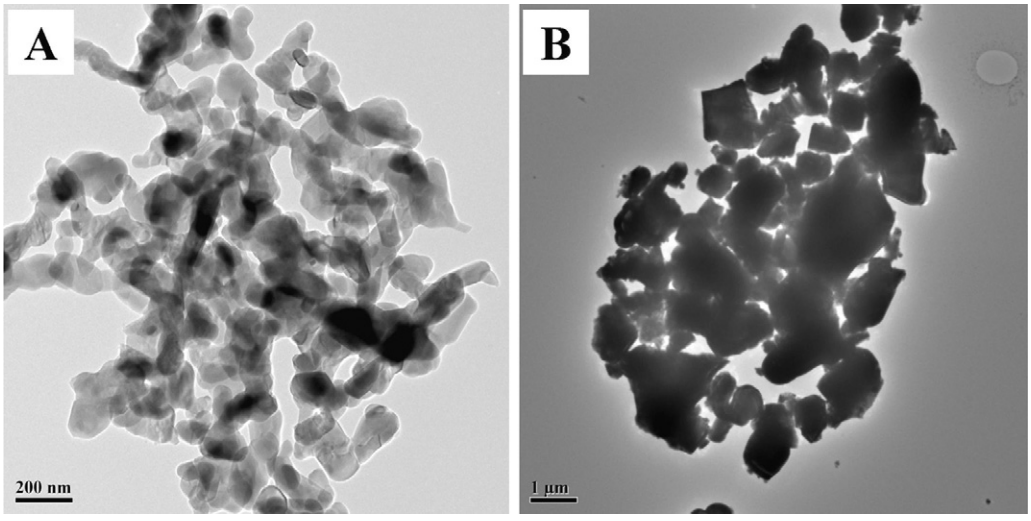

Fig. 1. FETEM micrographs of the β-TCP powders: synthetic nano-sized powders (A) and commercial micro-size powders (B).

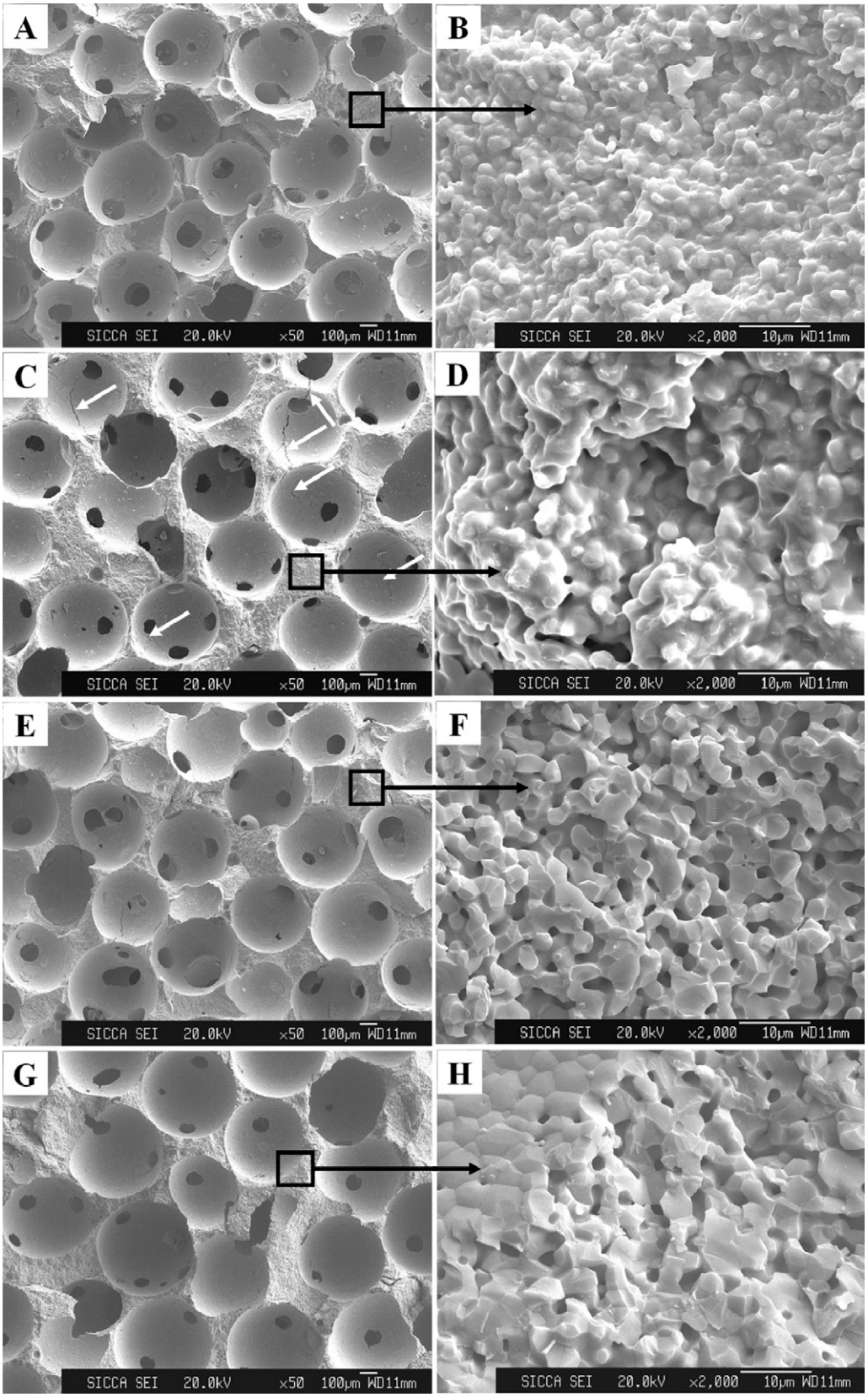

Fig. 3. FESEM micrograph of macroporous β-TCP scaffolds fabricated from synthetic nano-sized powders (A and B, sintered at 1100 °C; C and D, sintered at 1150 °C) and commercial micro-size powders (E and F, sintered at 1100 °C; G and H, sintered at 1150 °C).

Fig. 2 shows the XRD patterns of the synthetic and commercial powders. The results revealed that both of the powders were composed of highly crystalline and no second phase other than β-TCP.

Fig. 3 presents the FESEM micrographs of the fractured surface of the fabricated macroporous β-TCP scaffolds after sintering at different temperatures using different powders. The micrographs with low magnification show that all the samples were highly porous with evenly distributed and interconnected macropores. The shapes of macropores were similar to those of PMMA porogens, and the macropore size and interconnected pore size were about 400–550 μm and ~100 μm, respectively. At the same time, the micro-cracks (shown by white arrows in Fig. 3C) appeared in the sample sintered at 1150 °C from nano-powders, which was attributed to the phase transformation from β- to α-TCP (validated by XRD in Fig. 4). The microstructures of the solid walls in high magnifications (Fig. 3B, D, F and H) show the significant differences between the samples fabricated from different powders. It is clear to see that the solid walls of the samples fabricated from nano-powders had highly densified bodies with uniform grain shapes. With the increase of the sintering temperature from 1100 to 1150 °C, the average grain size increased from 1.6 to 2.7 μm. On the contrary, the solid wall of the samples fabricated from commercial micro-size powders showed much coarser and tortuous surface morphology with large numbers of intergranular micro-pores in the size of 0.5–2 μm. The decrease of the solid wall density resulted in the increase of the porosity of the fabricated samples, which was confirmed by the porosity data in Table 2. The average grain size of the samples sintered at 1100 and 1150 °C was 2.9 and 3.8 μm, respectively, which was apparently larger than those samples fabricated from nano-powders. At the same time, the micro-pore amount decreased slightly at the higher sintering temperature.

The difference in microstructures is directly related to the characteristics of the powders. Previous studies have shown that, as compared to the commercial micro-size powders, the nano-size powders with uniform grain size and less agglomeration have much higher driving force for densification due to the enormous surface area [27]. In the processes of ceramic sintering, as the sintering temperature increased, the driving force for densification and the rate of grain boundary motion increases, and breakaway of the boundaries from the pores and leaving of isolated pores in the grain interior occurs because the pores are slower moving than the grain boundaries [28]. Under the tension of a moving grain boundary, pores can move by volume or surface diffusion or even by evaporation–condensation across the pores [29]. In contrast, the pores in the ceramics fabricated from commercial micro-size powders with irregular grain size cannot be completely removed by rapid sintering rate and remain as closed pores, which limits the final densification [29]. On the other hand, the wide particle size distribution of the commercial micro-size powders with agglomerates and irregular morphology causes poor packing, which can also cause the exaggerated grain growth during sintering. The distinct microstructure characteristics of the scaffolds fabricated from different powders might result in quite different mechanical strength and other properties.

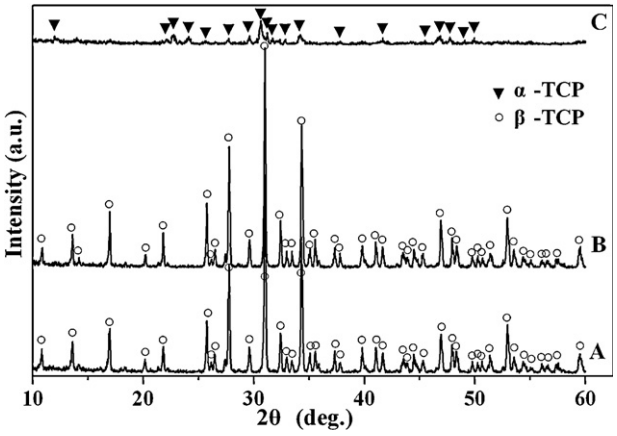

Fig. 4. XRD patterns of β-TCP bioceramics fabricated using nano-size and commercial micro-size powders: (A) nano-size powders sintered at 1100 °C, (B) commercial micro-size powders sintered at 1150 °C, and (C) nano-size powders sintered at 1150 °C.

Fig. 4 shows the XRD patterns of the samples sintered from the nano-size and commercial micro-size β-TCP powders. It can be seen that the samples fabricated from nano-size powders and sintered at 1100 °C were composed of highly crystalline and single-phase β-TCP, and no other phases were observed. When the sintering temperature increased to 1150 °C, β-TCP was completely transformed to α-TCP. In contrast, the β-TCP ceramics fabricated from commercial micro-size powders were maintained in β-phase even sintered at 1150 °C and no peaks of α-TCP were observed. Suggesting that the phase transition temperature of nano-size β-TCP powders is lower than that of commercially obtained commercial micro-size β-TCP powders. The previous studies have validated that the residual Mg and/or Fe content in β-TCP powders could increase the phase transition temperature from β- to α-TCP of the β-TCP materials [9]. In the present study, the residual Mg and Fe content in the commercial micro-size β-TCP powders were much higher than that in the synthetic nano-sized β-TCP powders (Table 1). Therefore, the phase transition from β- to α-

Table 2
Porosity and mechanical strength of the scaffolds fabricated from nano-size and micro-size β-TCP powders.

Samples	Porosity (%)	Compressive strength (MPa)	Elastic modulus (MPa)
Nanosize powders sintered at 1100 °C	64.86 ± 0.66	10.87 ± 1.36	1066.67 ± 221.21
Microsize powders sintered at 1100 °C	69.83 ± 1.10	5.48 ± 1.08	227.47 ± 32.29
Nanosize powders sintered at 1150 °C	64.83 ± 0.47	7.23 ± 0.96	222.43 ± 32.72
Microsize powders sintered at 1150 °C	68.70 ± 1.75	5.15 ± 0.79	209.43 ± 18.14

TCP appeared to happen at higher temperature for the scaffolds fabricated from commercial β-TCP powders than for that from the synthetic β-TCP powders.

Table 2 shows the porosity and mechanical properties of the β-TCP scaffolds fabricated from nano-size and commercial micro-size powders at 1100 °C and 1150 °C, respectively. It is clear to see that the compressive strength and elastic modulus of the samples fabricated from nano-size powders were much higher than those fabricated from commercial micro-size powders. The maximal value of the compressive strength of the scaffolds fabricated from nano-size β-TCP powders was almost twice as high as those fabricated from commercial micro-size β-TCP powders. The maximal compressive strength of the β-TCP bioceramic scaffolds fabricated by nano-size powders reached 10.87 MPa, which is comparable to the high end of compressive strength of cancellous bone (2–10 MPa) [30]. Based on the previous studies [31,32], the mechanical strength of the ceramics increases as the density increasing and grain size decreasing. Our results showed that employing nano-size β-TCP powders as raw materials could effectively increase the sintering density of the solid wall, avoiding the excessive growing of the grain size, obtaining fully dense and microstructural homogeneities of the β-TCP solid walls with fine grain size, and leading to higher mechanical strength.

Furthermore, for the samples fabricated from commercial micro-size β-TCP powders, an increase of the sintering temperature from 1100 °C to 1150 °C resulted in the decrease of the mechanical properties (compressive strength and elastic modules), which was due to the increase grain size at higher sintering temperature. However, the mechanical properties of the scaffolds fabricated from nano-size powders decreased obviously with the increase of the sintering temperature from 1100 °C to 1150 °C, which was caused by the phase transformation and accompanied appearing large amount of micro-creaks in the solid wall (Fig. 3C).

Degradation is another important requirement for the third-generation biomaterials [33]. Fig. 5 shows the degradation (weight loss percentage, wt.%) of the macroporous β-TCP scaffolds fabricated from nano-size and commercial micro-size powders and sintered at 1100 °C in Tris–HCl buffer solution. Degradation can be seen to increase with the increase of the soaking time. It is clear to see that the degradation of the samples sintered from nano-size powders only reached 0.46% at day 1. With the soaking time increasing, the degradation increased apparently, and reached 7.84% at day 14 and then increased step by step and reached 14.91% at day 21. In contrast, the degradation of the samples fabricated from commercial micro-size powders was much faster than those fabricated from nano-size powders. At day 1, it reached 0.69%. With the increase of the soaking time, the degradation increased sharply, and reached 19.24% at day 21. The results show that the extent of degradation of the scaffolds sintered from nano-size powders was just about three-fourths of those from commercial micro-size powders. The degradation rate of the biodegradable bioceramics is determined by many factors, such as sintering parameters, micro-pore structure and porosity. The micro-pores and porosity play dominant roles in the degradation of ceramics. With the increase of the micro-pore amount and porosity, the degradation rate increases apparently. Previous studies suggested that the degradation mechanism of the biodegradable bioceramics is mainly the solution dissolution, and the dissolution always occurs easily on the boundary of the open micro-pores [34–36]. The solid walls of the β-TCP scaffolds fabricated from nano-powders are almost fully dense. In contrast, the solid walls of the β-TCP scaffolds fabricated from commercial micro-size powders possessed large amount of micro-pores. Therefore, the degradation rate of the samples derived from commercial micro-size powders was apparently faster than those derived from nano-size powders, which indicated that the degradation of the β-TCP scaffolds also could be regulated by the initial powder size.

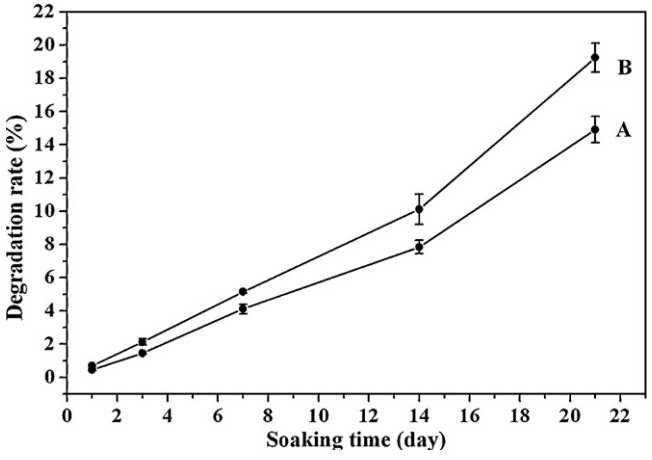

Fig. 5. Degradation of the β-TCP bioceramics sintered from nano-size (A) and commercial micro-size (B) powders at 1100 °C for 3 h.

4. Conclusions

In this study, the improvement of mechanical properties of macroporous β-TCP bioceramic scaffolds with uniform macropore size and interconnected pore structures were fabricated using nano-powders. The results showed that the sintering ability of the nano-size β-TCP powders was much higher than the commercial micro-size β-TCP powders. Using nano-size β-TCP powders as raw materials is an effective way to fabricate scaffolds with high mechanical properties. Using nano-size β-TCP powders, the maximal value of the compressive strength of the samples with a porosity of ∼65% reached 10.87 MPa, which was almost twice as high as those fabricated from commercial micro-size β-TCP powders and is comparable to the high-end value of cancellous bone. Furthermore, the degradation of the scaffolds sintered from nano-size powders was just about three-fourths of those from commercial micro-size powders, which indicated that the degradation of β-TCP scaffolds also could be regulated by the initial powder size. Regarding the porous structures and mechanical properties, the macroporous β-TCP bioceramic scaffolds fabricated from nano-powders could potentially be used in hard tissue regeneration and bone tissue engineering applications.

Acknowledgements

The authors gratefully acknowledge the support of K.C. Wong Education Foundation, Natural Science Foundation of China (Grant Nos.: 30900299 and 30730034), Science and Technology Commission of Shanghai Municipality (Grant No.: 0952nm04000) and Science Foundation for Youth Scholar of State Key Laboratory of High Performance Ceramics and Superfine Microstructures (Grant No.: SKL200902).

References

[1] T. Guda, M. Appleford, S. Oh, J.L. Ong, A cellular perspective to bioceramic scaffolds for bone tissue engineering: the state of the art, Curr. Top. Med. Chem. 8 (2008) 290–299.
[2] M. Mastrogiacomo, S. Scaglione, R. Martinetti, L. Dolcini, F. Beltrame, R. Cancedda, R. Quarto, Role of scaffold internal structure on in vivo bone formation in macroporous calcium phosphate bioceramics, Biomaterials 27 (2006) 3230–3237.
[3] R.E. Holmes, V. Mooney, R. Bucholz, A. Tencher, A coralline hydroxyapatite bone graft substitute: preliminary report, Clin. Orthop. Relat. Res. 188 (1984) 252–262.
[4] E. Wintermantel, J. Mayer, K.L. Blum, P. Eckert, P. Luscher, M. Mathey, Tissue engineering scaffolds using superstructures, Biomaterials 17 (1996) 83–91.
[5] M. Bohner, F. Baumgart, Theoretical model to determine the effects of geometrical factors on the resorption of calcium phosphate bone substitutes, Biomaterials 25 (2004) 3569–3582.
[6] M. Maddalena, S. Silvia, M. Roberta, D. Laura, B. Francesco, C. Ranieri, Q. Rodolfo, Role of scaffold internal structure on in vivo bone formation in macroporous calcium phosphate bioceramics, Biomaterials 27 (2006) 3230–3237.
[7] F. Bai, Z. Wang, J.X. Lu, J. Liu, G.Y. Chen, R. Lv, J. Wang, K.L. Lin, J.K. Zhang, X. Huang, The correlation between the internal structure and vascularization of controllable porous bioceramic materials in vivo: a quantitative study, Tissue Eng. 16A (2010) 3791–3803.
[8] S.V. Dorozhkin, Calcium orthophosphates, J. Mater. Sci. 42 (2007) 1061–1095.
[9] J.C. Elliot, Structure and Chemistry of the Apatites and Other Calcium Orthophosphates, Elsevier, Amsterdam, 1994.
[10] Y.H. Kim, M.A. Jyoti, M.H. Youn, H.S. Youn, H.S. Seo, B.T. Lee, H.Y. Song, In vitro and in vivo evaluation of a macro porous beta-TCP granule-shaped bone substitute fabricated by the fibrous monolithic process, Biomed. Mater. 5 (2010) 035007.
[11] R.B. Santana, C.M.L. De Mattos, T. Van Dyke, Efficacy of combined regenerative treatments in human mandibular class II furcation defects, J. Periodontol. 80 (2009) 1756–1764.
[12] L.L. Hench, Bioceramics, J. Am. Ceram. Soc. 81 (1998) 1705–1728.
[13] K. Groot, Clinical applications of calcium phosphate biomaterials: a review, Ceram. Int. 19 (1993) 363–366.
[14] R. Cancedda, P. Giannoni, M. Mastrogiacomo, A tissue engineering approach to bone repair in large animal models and in clinical practice, Biomaterials 28 (2007) 4240–4250.
[15] H.R.R. Ramay, M. Zhang, Biphasic calcium phosphate nanocomposite porous scaffolds for load-bearing bone tissue engineering, Biomaterials 25 (2004) 5171–5180.
[16] P. Ducheyne, Bioceramics: material characteristic versus in vivo behavior, J. Biomed. Mater. Res. 21 (1987) 219–236.
[17] M.J. Yaszemski, R.G. Payne, W.C. Hayes, R. Lander, A.G. Mikos, Evolution of bone transplantation: molecular, cellular and tissue strategies to engineer human bone, Biomaterials 17 (1996) 175–185.
[18] M. Jarcho, R.L. Salisbury, M.B. Thomas, R.H. Doremus, Synthesis and fabrication of β-tricalcium phosphate ceramics for potential prosthetic application, J. Mater. Sci. 14 (1979) 142–150.
[19] F.H. Perera, F.J. Martínez-Vázquez, P. Miranda, A.L. Ortiz, A. Pajares, Clarifying the effect of sintering conditions on the microstructure and mechanical properties of β-tricalcium phosphate, Ceram. Int. 36 (2010) 1929–1935.
[20] K.L. Lin, J. Chang, J.X. Lu, J.H. Gao, Y. Zeng, Properties of β-$Ca_3(PO_4)_2$ bioceramics prepared using nano-size powders, Ceram. Int. 33 (2007) 979–985.
[21] F.M. Zhang, J. Chang, K.L. Lin, J.X. Lu, Preparation, mechanical properties and in vitro degradability of wollastonite/tricalcium phosphate macroporous scaffolds from nanocomposite powders, J. Mater. Sci. Mater. Med. 19 (2008) 167–173.
[22] M. Descamps, T. Duhoo, F. Monchaua, J. Lu, P. Hardouin, J.C. Hornez, Manufacture of macroporous β-tricalcium phosphate bioceramics, J. Eur. Ceram. Soc. 28 (2008) 149–157.
[23] M. Descamps, O. Richart, P. Hardouin, J.C. Hornez, A. Leriche, Synthesis of macroporous β-tricalcium phosphate with controlled porous architectural, Ceram. Int. 34 (2008) 1131–1137.
[24] L.J. Gibson, M.F. Ashby, Cellular Solids: Structure and Properties, second ed., Cambridge University Press, 1997,, p. 15.
[25] N. Bouslama, F.B. Ayed, J. Bouaziz, Effect of fluorapatite additive on densification and mechanical properties of tricalcium phosphate, J. Mech. Behav. Biomed. Mater. 3 (2010) 2–13.
[26] K.L. Lin, J. Chang, Z. Wang, Fabrication and the characterisation of the bioactivity and degradability of macroporous calcium silicate bioceramics in vitro, J. Inorg. Mater. 20 (2005) 692–698.
[27] A.S. Edelstein, R.C. Cammarata (Eds.), Nanomaterials: Synthesis, Properties and Applications, Institute of Physics (IOP), Bristol, England, 1996
[28] R.J. Brook, Pore and grain growth kinetics, J. Am. Ceram. Soc. 52 (1969) 339–340.
[29] D.W. Richerson (Ed.), Modern Ceramic Engineering: Properties, Processing and Use in Design, Marcel Dekker, New York, 1922.
[30] L.J. Gibson, The mechanical behavior of cancellous bone, Biomechanics 18 (1985) 317–328.
[31] F.P. Knudsen, Dependence of mechanical strength of brittle polycrystalline specimens on porosity and grain size, J. Am. Ceram. Soc. 42 (1959) 376–387.
[32] K.B. Lunde, B. Skallerud, The modified cam clay model for constrained compression of human morsellised bone: effects of porosity on the mechanical behaviour, J Mech. Behav. Biomed. Mater. 2 (2009) 43–50.
[33] L.L. Hench, J.M. Polak, Third-generation biomedical materials, Science 295 (2002) 1014–1017.
[34] J.X. Lu, M. Descamps, J. Dejou, G. Koubi, P. Hardouin, J. Lemaitre, J.P. Proust, The biodegradation mechanism of calcium phosphate biomaterials in bone, J. Biomed. Mater. Res. 63 (2002) 408–412.
[35] H.K. Koerten, J. Meulen, Degradation of calcium phosphate ceramics, J. Biomed. Mater. Res. 44 (1999) 78–86.
[36] C.P.A.T. Klein, A.A. Driessen, K. Groot, Biodegradation behavior of various calcium phosphate materials in bone tissue, J. Biomed. Mater. Res. 17 (1983) 769–784.